International Journal of Engineering, Mathematical and Physical Sciences
ISSN: 2517-9934
Vol:8, No:3, 2014

The Effect of the Crystal Field Interaction on the Critical Temperatures and the Sublattice Magnetizations of a Mixed Spin-3/2 and Spin-5/2 Ferrimagnetic System

Fathi Abubrig, Mohamed Delfag, Suad M. Abuzariba

Abstract**—**The influence of the crystal field interactions on the mixed spin-3/2 and spin-5/2 ferrimagnetic Ising system is considered by using the mean field theory based on Bogoliubov inequality for the Gibbs free energy. The ground-state phase diagram is constructed, the phase diagrams of the second-order critical temperatures are obtained, and the thermal variation of the sublattice magnetizations is investigated in detail. We find some interesting phenomena for the sublattice magnetizations at particular values of the crystal field interactions.

Keywords**—**Crystal field, Ising system, Ferrimagnetic, magnetization, phase diagrams.

I. Introduction

THE Ising model, with high and mixed spins, is an interesting subject of study because of its observed critical behaviors. The two sublattice mixed Ising ferrimagnetic systems have been of interest in the last two decades, for not only purely theoretical purposes but also because they have been proposed as possible systems to describe ferromagnetic and ferrimagnetic materials [1]. Moreover, the increasing interest in these systems is mainly related to the technological applications of these systems in the area of thermomagnetic recording [2]. Since the mixed spin Ising systems have less translational symmetry than their single spin counterparts, they exhibit many new phenomena which cannot be observed in the single-spin Ising systems and the study of these systems can be relevant for understanding of bimetallic molecular systems based magnetic materials [3].

One of the earliest and simplest of these models to be studied was the mixed spin Ising system consisting of spin-1/2 and spin-S (S > 1/2) in a uniaxial crystal field. The model for different values of S (S > 1/2) has been investigated by exact (on honeycomb lattice [4]-[6], as well as on Bethe lattice [7], [8], mean field approximation [9], effective field theory with correlations [10]-[14], cluster variational theory [8], renormalization-group technique [15] and Monte-Carlo simulation [16]-[18]. The mixed- spin Ising systems consisting of higher spins are not without interest. Indeed, the magnetic properties of mixed spin-1 and spin-3/2 Ising ferromagnetic system with different single-ion anisotropies have been investigated with the use of an effective field theory [18], [19], mean field theory [20], a cluster variational method [21] and Monte Carlo simulation [22].

Recently, the investigations have been extended to high order mixed spin ferrimagnetic systems (mixed spin-3/2 and spin-2 ferrimagnetic system and mixed spin-3/2 and spin-5/2) in order to construct their phase diagrams in the temperature-anisotropy plane and to consider magnetic properties of these systems. Bobak and Delay investigated the effect of single-ion anisotropy on the phase diagram of the mixed spin-3/2 and spin-2 Ising system by the use of a mean-field theory based on the Bogoliubov inequality for the free energy [23]. Albayrak [24] studied the critical behaviour of the mixed spin-2 and spin-5/2 Ising ferrimagnetic system on Bethe lattice and he also [25] examined the critical and the compensation temperatures of the mixed spin-2 and spin-5/2 Ising ferrimagnetic system on Bethe lattice by using the exact recursion equations. Bayram Deviren et al. have used the effective field theory to study the magnetic properties of the ferrimagnetic mixed spin-3/2 and spin-2 Ising model with crystal field in a longitudinal magnetic field on a honeycomb and a square lattice [26].

In this paper, our aim is to consider a mixed spin-3/2 and spin-5/2 ferrimagnetic system within the framework of the mean-field theory based on Bogoliubov inequality for the Gibbs free energy, in order to investigate the influence of the crystal-field interaction on the critical temperatures and to find the change in the sublattice magnetizations of the system as a function of the temperature at a different values of the crystal-field interaction.

This paper is organized as follows: Section II briefly presents the mixed spin Ising model and its mean-field solution. Section III gives the results and the discussions. In Section IV the conclusion is summarized.

II. The Model and Calculation

We consider a mixed Ising spin-2 and spin-5/2 system consisting of two sublattices *A* and *B*, which are arranged alternately. The sublattice *A* are occupied by spins S_i , which

Fathi Abubrig is with the Physics Department, Faculty of science, Elmergeb University, Zliten, Libya (e-mail: Dr_fathiomar@yahoo.com).
Mohamed Delfag is with the Physics Department, Faculty of Education, Misurata University, Libya (e-mail: msdelfag@yahoo.com).
Suad M Abuzariba is with the Physics Department, Faculty of Science, Misurata University (e-mail: suadabu@yahoo.com).

take the spin values of $\pm 3/2, \pm 1/2$, while the sublattice *B* are occupied by spins S_j, which take the spin values of . $\pm 5/2, \pm 3/2, \pm 1/2$. In each site of the lattice, there is a single-ion anisotropy D_A in the sublattices *A* and D_B in the sublattice *B*) acting in the spin-3/2 and spin-5/2. The Hamiltonian of the system according to the mean-field theory is given by

$$H = -J \sum_{(i,j)} S_i^A S_j^B - D_A \sum (S_i^A)^2 - D_B \sum (S_j^B)^2, \quad (1)$$

where the first summation is carried out only over nearest-neighbor pairs of spins on different sublattices and *J* is the nearest-neighbour exchange interaction.

The most direct way of deriving the mean-field theory is to use the variation principle for the Gibbs free energy,

$$G(H) \le \Phi \equiv G_0(H_0) + \langle H - H_0 \rangle_0, \quad (2)$$

where $G(H)$ is the true free energy of the model described by Hamiltonian given in (1), $G_0(H)$ is the model described by the trial Hamiltonian H_0 which depends on variational parameters and $\langle \cdots \rangle_0$ denotes a thermal average over the ensemble defined by H_0.

Now, depending on the choice of the trial Hamiltonian, one can construct approximate methods of different accuracy. However, owing to the complexity of the problem, we consider in this work the simple choice of H_0, namely

$$H_0 = -\sum_{i \in A} [\gamma_A S_i^A + D_A (S_i^A)^2] - \sum_{j \in B} [\gamma_B S_j^B + D_B (S_j^B)^2], \quad (3)$$

where γ_A and γ_B are the two variational parameters related to the molecular fields acting on the two different sublattices, respectively.

By evaluating (2), it is easy to obtain the expression of the free energy per site in *MFA*,

$$g = \frac{\phi}{N} = \frac{-1}{2\beta} \left[\ln \left(\exp\left(\frac{25}{4}\beta D_A\right) \left(2\cosh \frac{5}{2}\beta\gamma_A + \exp\left(-4\beta D_A\right) \left(2\cosh \frac{3}{2}\beta\gamma_A \right) + \exp\left(-6\beta D_A\right) \left(2\cosh \frac{1}{2}\beta\gamma_A \right) \right) \right) \right.$$
$$\left. + \ln \left(\exp\left(\frac{9}{4}\beta D_B\right) \left(2\cosh \frac{1}{2}\beta\gamma_B + \exp\left(-2\beta D_B\right) \left(2\cosh \frac{1}{2}\beta\gamma_B \right) \right) \right) \right] + \frac{1}{2}\left(zJ m_B m_A\right) \quad (4)$$

$$m_A = \frac{1}{2} \left[\frac{5\sinh\left(\frac{5}{2}\beta\gamma_B\right) + 3\exp(-4\beta D_B)\sinh\left(\frac{3}{2}\beta\gamma_B\right) + \exp(-6\beta\gamma_B)\sinh\left(\frac{1}{2}\beta\gamma_B\right)}{\cosh\left(\frac{5}{2}\beta\gamma_B\right) + \exp(-4\beta D_B)\cosh\left(\frac{3}{2}\beta\gamma_B\right) + \exp(-6\beta D_B)\cosh\left(\frac{1}{2}\beta\gamma_B\right)} \right] \quad (5)$$

$$m_B = \frac{3\sinh\left(3/2\ \beta\gamma_B\right) + \exp(-2\beta D_B)\sinh\left(1/2\beta\gamma_B\right)}{2\cosh\left(3/2\ \beta\gamma_B\right) + 2\exp(-2\beta D_B)\cosh\left(1/2\beta\gamma_B\right)} \quad (6)$$

where $\beta = 1/k_B T$, *N* is the total number of sites of the lattice and z is the number of the nearest neighbors of every ion in the lattice m_A and m_B are the sublattice magnetizations per site which are defined by (5).

Now, by minimizing the free energy (4) with respect to γ_A and γ_B, we obtain

$$\gamma_A = zJ\, m_B, \quad \gamma_B = zJ\, m_A. \quad (7)$$

The mean-field properties of the present model are then given by (4)-(7). Since (5)-(7) have in general several solutions for the pair (m_A, m_B), the stable phase will be the one which minimizes the free energy. When the system undergoes the second-order transition from an ordered state $(m_A \neq 0, m_B \neq 0)$, to the paramagnetic state $(m_A = 0, m_B = 0)$, this part of the phase diagram can be determined analytically. Because the magnetizations m_A and m_B are very small in the neighborhood of second-order transition point, we can expand (4)-(6) to obtain a Landau-like expansion. In this way, critical and tricritical points are determined according to the following routine;

1) Second-order transition lines when a=0 and b>0;
2) Tricritical points, if they are exist, when a=b=0, and c > 0.

III. Results and Discussions

A. Ground State Phase Diagram

Before going into the detailed calculation of the phase diagram of the model at higher temperature, let us first investigate the ground state structure of the model at zero temperature analytically. The ground-state phase diagram is easily determined from Hamiltonian Equation (1) by comparing the ground-state energies of the different phases, then the ground state configuration is the one with the lowest energy and each of these configurations for the given system parameters correspond to the stable states of the model which are indicated in Fig. 1.

At zero temperature, we find six phases with different values of $\{m_A, m_B, q_A, q_B\}$, namely the ordered ferrimagnetic phases.

These ordered phases are separated by first ordered lines and the values of $\{m_A, m_B, q_A, q_B\}$ for these phases are given as following:

$$O_1 = \left(\frac{5}{2}, \frac{-3}{2}, \frac{25}{4}, \frac{9}{4}\right),\ O_2 = \left(\frac{5}{2}, \frac{-1}{2}, \frac{25}{4}, \frac{1}{4}\right),$$
$$O_3 = \left(\frac{3}{2}, \frac{-3}{2}, \frac{9}{4}, \frac{9}{4}\right), O_4 = \left(\frac{3}{2}, \frac{-1}{2}, \frac{9}{4}, \frac{1}{4}\right),$$
$$O_5 = \left(\frac{1}{2}, \frac{-3}{2}, \frac{1}{4}, \frac{9}{4}\right),\ O_6 = \left(\frac{1}{2}, \frac{-1}{2}, \frac{1}{4}, \frac{1}{4}\right).$$

where the parameters q_A and q_B are defined by:

$$q_A = \langle S_i^A \rangle^2 \quad \text{and} \quad q_B = \langle S_j^B \rangle^2$$

It should be mentioned that, in this mixed-spin-system, the ground- state phase diagram exhibit no disordered phases and that the ground state phase diagram is very important in classifying the different phase regions of the model for the phase diagrams at higher temperatures.

B. Finite Temperature Phase Diagrams

In Figs. 2 and 3, the second-order critical temperature lines which separate the ordered phases, i.e. ferrimagnetic phases, from the paramagnetic phase of the mixed spin-3/2 and the spin-5/2 Ising ferrimagnetic system are depicted in the $(D_A / z|J|, k_B T_c / z|J|)$ and $(D_B / z|J|, k_B T_c / z|J|)$ planes for some selected values of $D_A/z|J|$ for spin-5/2 and $D_B / z|J|$ for spin-3/2, respectively.

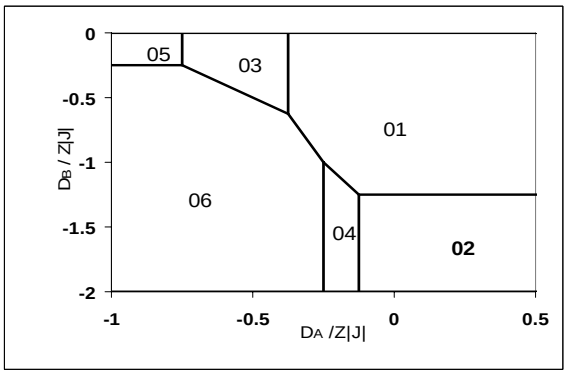

Fig. 1 Ground-state phase diagram of the mixed spin-3/2 and spin-5/2 Ising ferrimagnetic system with the coordination number z and different single-ion anisotropies $D_A / z|J|$ and $D_B / z|J|$ The four phases: ordered O_1, O_2, O_3, O_4, O_5, O_6 and there are no disordered phases in the ground-state phase diagram

The second-order critical temperature lines are easily obtained by setting $a = 0$ and $b > 0$. The first phase diagram is obtained on the $(D_B / z|J|, k_B T_c / z|J|)$ plane and presented in Fig. 2. This phase diagram shows the general characteristics of the model for given values of $D_A/z|J|$ in the range $-6.0 < D_A/z|J| < 6.0$. In this figure, one can observe that this mixed spin system exhibits second-order critical temperature lines only and does not exhibit any tricritical points or first order critical temperature lines, indicating that this system has no first order phase transition.

It is also obvious that the second-order lines corresponding to each value of $D_A/z|J|$ present two straight portions at lower and higher temperatures for the low negative and high positive values of $D_B/z|J|$, respectively, meaning that the critical temperatures of the model become constant in these limits. These two straight portions of the second-order lines combine with each other with a gradually increasing part. At this part, the values of the second-order critical temperatures increase rapidly by increasing the values of $D_B/z|J|$, then, they start to increase slowly until they come to the highest saturated value at high positive values of $D_B/z|J|$.

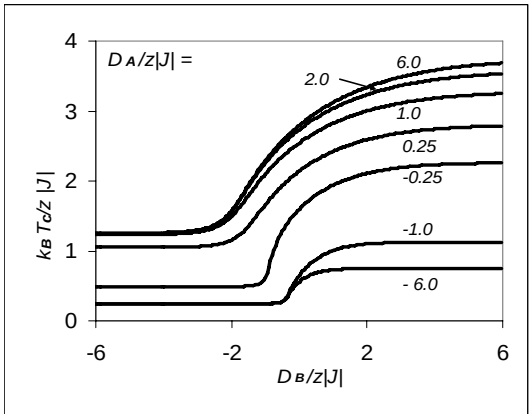

Fig. 2 Phase diagram in the (D_B, T) plane for the mixed-spin Ising ferrimagnet with the coordination number z, when the value of $D_A / z \mid J \mid$ is changed

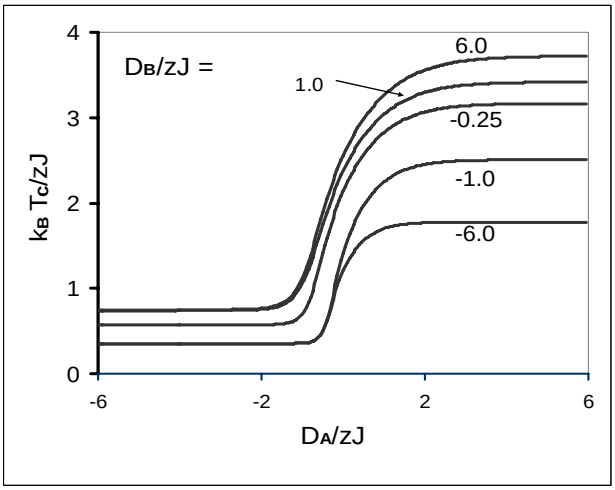

Fig. 3 Phase diagram in the (D_A, T) plane for the mixed-spin Ising ferrimagnet with the coordination number z, when the value of $D_B / z \mid J \mid$ is changed

On the other hand, at this part, the second-order critical temperatures values decrease rapidly by decreasing the values of $D_B / z \mid J \mid$, then they start to decrease slowly until they come to the lowest saturated value at low negative values of $D_B / z \mid J \mid$.

The second phase diagram is obtained on the $(D_A / z \mid J \mid, k_B T_c / z \mid J \mid)$ plane for selected values of $D_B / z \mid J \mid$ in the range $-6.0 < D_B / z \mid J \mid < 6.0$ and is depicted in Fig. 3. From this figure, it is clear that the behavior of the second order critical temperature lines with $D_A / z \mid J \mid$ for different values of $D_B / z \mid J \mid$ is similar to their behavior with $D_B / z \mid J \mid$ for different values of $D_A / z \mid J \mid$ which is depicted in Fig. 2.

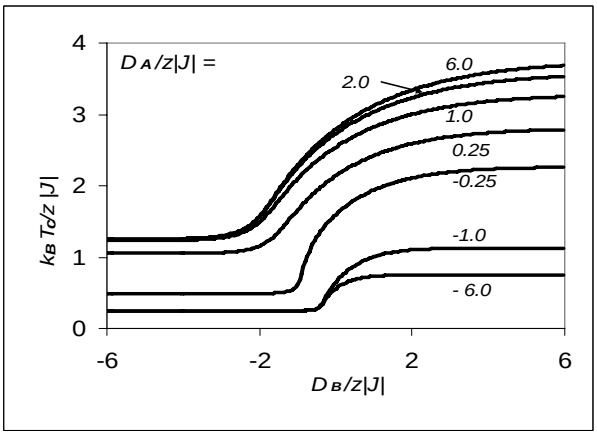

Fig. 4 Phase diagram in the (D_B, T) plane for the mixed-spin Ising ferrimagnet with the coordination number z, when the value of $D_A / z \mid J \mid = 20$ and $D_A / z \mid J \mid = -20$. The saturated values of the second-order critical temperatures are shown in this figure

For the final illustrations, let us now turn our attention to the saturated values of the critical temperatures for high values and low values of $D_A / z \mid J \mid$ and $D_B / z \mid J \mid$. As shown in Fig. 4, for high positive and negative values of $D_A / z \mid J \mid$ and $D_B / z \mid J \mid$. When $D_A / z \mid J \mid \to \infty$ and $D_B / z \mid J \mid \to \infty$, the saturated value of the critical temperatures is $k_B T_c / z \mid J \mid = 3.75$. When $D_A / z \mid J \mid \to \infty$ and $D_B / z \mid J \mid \to -\infty$, the saturated value of the critical temperatures is $k_B T_c / z \mid J \mid = 1.25$. When $D_A / z \mid J \mid \to -\infty$ and $D_B / z \mid J \mid \to \infty$, the saturated value of the critical points is. $k_B T_c / z \mid J \mid = 0.75$. If $D_A / z \mid J \mid \to -\infty$ and $D_B / z \mid J \mid \to -\infty$, the saturated value is $k_B T_c / z \mid J \mid = 0.25$.

C. Sublattice Magnetizations m_A and m_B.

In this subsection, let us at first examine the temperature dependence of the sublattice magnetizations m_A and m_B for the system. The results are depicted in Figs. 5- 7.

Fig. 5 shows typical sublattice magnetization curves with $D_B / z \mid J \mid = 1.0$, and selected values of $D_A / z \mid J \mid$. In this case, all the sublattice magnetization curves have standard characteristic convex shape. Moreover, in the present system and for all the values of the crystal field interactions $D_A / z \mid J \mid$ and $D_B / z \mid J \mid$, the present system exhibits second-order phase transitions only, consequently, the sublattice magnetizations decrease by increasing temperature from their

saturation values at $T = 0\ K$ and vanish continuously at the critical temperatures T_c.

By comparing the values of the sublattice magnetizations at zero temperature, for different values of $D_A/z|J|$ and $D_B/z|J|$ in Fig. 5 with the values of the sublattice magnetizations, corresponding to the different phases and to the boundary between the phases, at the ground-state phase diagram (Fig. 1), we find that they are in an agreement and every sublattice magnetization has the same saturated value at $T = 0\ K$ as in the ground state phase diagram.

In Figs. 6 and 7, we turn our attention to the points which are located close to or at the boundaries between the phases in the ground-state phase diagram. In Fig. 6, when $D_B/z|J| = 1.0$ and $D_A/z|J| = -0.35$ (this point located in the ordered phase O_1 and close to the boundary between the ordered phase O_1 and the ordered phase O_3 in the ground state phase diagram, where $D_A/z|J| = -0.375$). In this case, the temperature dependences of m_A may exhibit a rather rapid decrease (damping) from its saturation value at $T = 0\ K$. The phenomena is further enhanced when the value of $D_A/z|J|$ approaches the boundary. At $D_B/z|J| = -0.375$ (at the boundary) and for $T = 0\ K$, the saturation value of m_A is $m_A = 2.0$, which indicates that in the ground state the spin configuration of S_j^B in the system consists of the mixed state; in this state half of the spins on sublattice *B* are equal to +5/2 (or -5/2) and the other half are equal to +3/2 (or -3/2).

By further decreasing $D_A/z|J|$, the ground state becomes O_3, with $m_A = 3/2$ at $T = 0\ K$. In this region, when $D_A/z|J| = -0.4$ (slightly below the boundary between the ordered phases O_1 and O_3) the thermal variation of m_A exhibits an interesting feature which is the initial rise (excitation) of m_A with the increase of temperature before decreasing to zero at the critical point. On the other hand, for all values of $D_A/z|J|$.

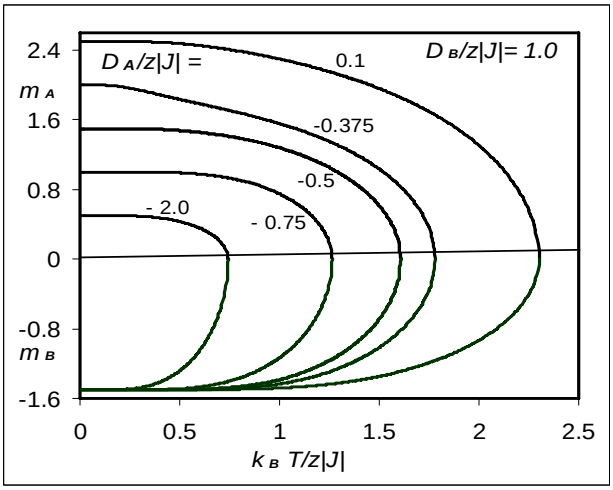

Fig. 5 Thermal variation of the sublattice magnetizations m_A, m_B for the mixed-spin Ising ferrimagnet with the coordination number z, when the value of $D_A/z|J|$ is changed for fixed $D_B/z|J| = 1.0$

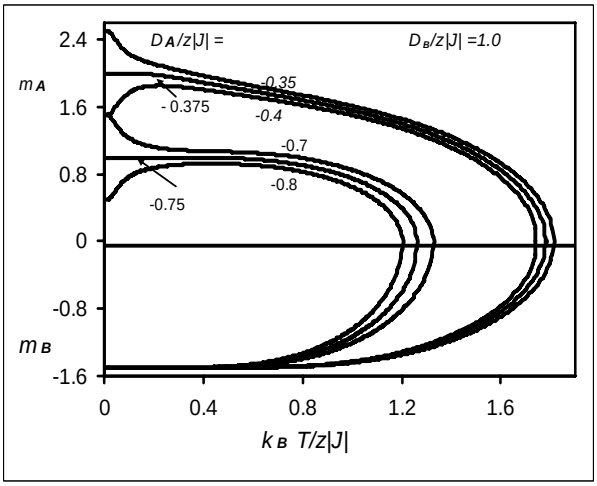

Fig. 6 Thermal variation of the sublattice magnetizations m_A, m_B for the mixed-spin Ising ferrimagnet with the coordination number z, when the value of $D_A/z|J|$ is changed for fixed $D_B/z|J| = 1.0$

In Fig. 6 and for all these values of $D_A/z|J|$ the sublattice magnetization m_B may show normal behavior even though it is coupled to m_A.

When $D_B/z|J|$ has the values $-0.7, -0.75$ and -0.8 (close to and at the boundary between the ordered-phases O_3 and O_5 in the ground-state phase diagram), it is clear from Fig. 6 that the temperature dependences of m_B and m_A exhibit similar behaviors to the temperature dependences of m_B and m_A in the previous case.

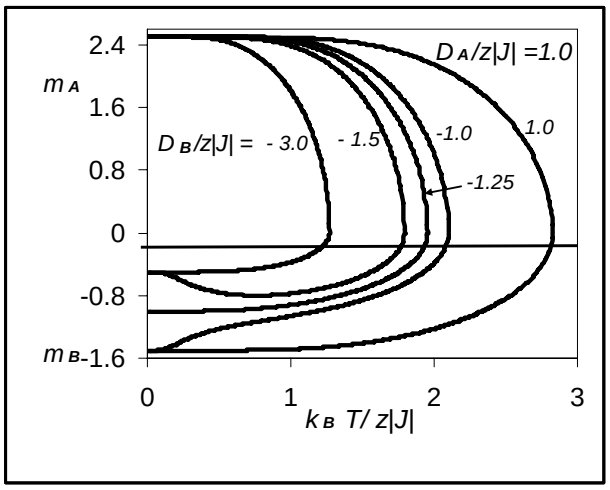

Fig. 7 Thermal variation of the sublattice magnetizations m_A, m_B for the mixed-spin Ising ferrimagnet with the coordination number z, when the value of $D_B / z|J|$ is changed for fixed $D_A / z|J| = 1.0$

Fig. 7 shows the sublattice magnetization curves as a function of temperature for several values of $D_B / z|J|$, when $D_A / z|J| = 1.0$. In this case, the selection of $D_B / z|J|$ corresponds to the crossover from the O_1 to the O_3 phase. When $D_B / z|J| = 1.0$, the sublattice magnetization m_B may show normal behavior. When $D_B / z|J| = -1.0$ (slightly above the boundary between the ordered phase O_1 and the ordered phase O_2, where $D_B / z|J| = -1.0$) the magnetization curve m_B may exhibit a rather rapid decrease from its saturation value $(m_B = -3/2)$ at $T = 0\ K$, while for the value of $D_B / z|J| = -1.5$ (slightly below that boundary), there is a rapid increase of m_B from the saturation value $(m_B = -1/2)$ with the increase in *T*.

When the value of $D_B / z|J| = -1.25$, the saturation value of the sublattice magnetization m_B at $T = 0\ K$ is $(m_B = -1.0)$. It indicates that at this point, the spin configuration of S_j^B in the ground state consists of the mixed state; half of the spins on the sublattice *B* are equal to -3/2 (or +3/2 as well) and the other half are equal to -1/2 (or +1/2 as well). It is also seen from Fig. 7 that when $D_B / z|J| = -3.0$, the sublattice magnetization m_B decreases normally from its saturation value $(m_B = -1/2)$ to vanish at the critical temperature T_c. On the other hand, for all values of $D_B / z|J|$ the sublattice magnetization m_A may show normal behavior, even though it is coupled to m_B.

IV. Conclusions

In this work, we have studied The effect of the crystal field interactions on the critical temperatures and the sublattice magnetizations of a mixed spin-3/2 and spin-5/2 ferrimagnetic system by using the mean-field theory based on Bogoliubov inequality for the Gibbs free energy. Some new results on the phase diagrams and the sublattice magnetization curves have been obtained. We obtain six ordered Phases in the ground state phase diagram. We have found that the ground-state phase diagram for this system does not exhibit disordered phases. The finite temperature phase diagrams exhibit only second-order critical temperature lines. We found that for the values of the crystal field interactions close to the boundaries between the phases in the ground state phase diagram, the sublattice magnetization curves for this system may exhibit a rapid increase or decrease in their values by increasing the temperature before the sublattice magnetizations vanish at the critical points.

References

[1] Drillon M, Coronado E, Beltran D, Georges R. Classical treatment of a heisenberg linear chain with spin alternation; application to the MnNi(EDTA)·6H_2O complex. Chem Phys, 1983, 79: 449-453.
[2] M. Mansuripur, "Magnetization Reversal, Coercivity, and the Process of Thermomagnetic Recording in Thin Films of Amorphous Rare Earth Transition Metal Alloys," Journal of Applied Physics, Vol. 61, No. 4, 1987, pp. 1580-1587.
[3] O. Kahn, in: E. Coronado, et al., (Eds.), Molecular Magnetism: From Molecular Assemblies to the Devices, Kluwer Academic Publishers, Dordrecht, 1996.
[4] L. L. Goncaloves, "Uniaxial Anisotropy Effects in the Ising Model: An Exactly Soluble Model," Physica Scripta, Vol. 33, No. 2, 1986, p. 192.
[5] A. Dakhama and N. Benayad, "On the Existence of Compensation Temperature in 2d Mixed-Spin Ising Ferri magnets: An Exactly Solvable Model," Journal of Magnetism and Magnetic Materials, Vol. 213, No. 1-2, 2000, pp. 117-125.
[6] N. R. da Silva and S. R. Salinas, "Mixed-Spin Ising Model on Beth Lattice," Physical Review, Vol. 44, No. 2, 1991, pp. 852-855.
[7] J. W. Tucker, "The Ferrimagnetic Mixed Spin-1/2 and Spin-1 Sing System," Journal of Magnetism and Magnetic Materials, Vol. 195, No. 3, 1999, pp.
[8] T. Kaneyoshi and J. C. Chen, "Mean-Field Analysis of a Ferrimagnetic Mixed Spin System," Journal of Magnet ism and Magnetic Materials, Vol. 98, No. 1-2, 1991, pp. 201-204.
[9] T. Kaneyoshi, "Curie Temperatures and Tricritical Points in Mixed Ising Ferromagnetic Systems," The Physical Society of Japan, Vol. 56, 1987, pp. 2675-2680. doi:10.1143/JPSJ.56.2675.
[10] T. Kaneyoshi, "Phase Transition of the Mixed Spin System with a Random Crystal Field," Physica A, Vol. 153, No. 3, 1988, pp. 556-566..
[11] T. Kaneyoshi, M. Jascur and P. Tomczak, "The Ferri magnetic Mixed Spin-1/2 and Spin-3/2 Ising System," Journal of Physics: Condensed Matter, Vol. 4, No. 49, 1992, pp. L653-L658.
[12] T. Kaneyoshi, "Tricritical Behavior of a Mixed Spin-1/2 and Spin-2 Ising System," Physica A, Vol. 205, No. 4, 1994, pp. 677-686.
[13] A. Bobak and M. Jurcisin, "Discussion of Critical Behaviour in a Mixed-Spin Ising Model," Physica A, Vol. 240, No. 3-4, 1997, pp. 647-656.
[14] S. G. A. Quadros and S. R. Salinas, "Renormalization Group Calculations for a Mixed-Spin Ising Model," Physica A: Statistical Mechanics and Its Applications, Vol. 206, No. 3-4, 1994, pp. 479-496.
[15] G. M. Zhang, Ch.Z. Yang, "Monte Carlo Study of the Two-Dimensional Quadratic Ising Ferromagnet with Spins S = 1/2 and S = 1 and with Crystal-Field Interactions," *Physical Review B*, Vol. 48, No. 13, 1993, pp. 9452-9455.
[16] G. M. Buendia and M. A. Novotny, "Numerical Study of a Mixed Ising Ferrimagnetic System," Journal of Physics: Condensed Matter, Vol. 9, No. 27, 1997, pp. 5951-5964.

[17] G. M. Buendia and J. A. Liendo, "Monte Carlo Simulation of a Mixed Spin-1/2 and Spin-3/2 Ising Ferrimagnetic System," Journal of Physics: Condensed Matter, Vol. 9, No. 25, 1997, pp. 5439-5448.
[18] Bobak, "The Effect of Anisotropies on the Magnetic Pro perties of a Mixed Spin-1 and Spin-3/2 Ising Ferrimag netic System," Physica A, Vol. 258, No. 1-2, 1998, pp. 140-156.
[19] A. Bobak, O. F. Abubrig and D. Horvath, "An Effective-Field Study of the Mixed Spin-1 and Spin-3/2 Ising Ferrimagnetic System," Journal of Magnetism and Magnetic Materials, Vol. 246, No. 1-2, 2002, pp. 177-183.
[20] O. F. Abubrig, D. Horváth, A. Bobák and M. Jaščur, Mean-field solution of the mixed spin-1 and spin-3/2 Ising system with different single-ion anisotropies, *Physica A* 296 (2001) 437-450.
[21] J. W. Tucker, "Mixed Spin-1 and Spin-3/2 Blume-Capel Ising Ferromagnet," Journal of Magnetism and Mgnetic Materials, Vol. 237, No. 2, 2001, pp. 215-224.
[22] Y. Nakamura and J. W. Tucker. Monte Carlo study of a mixed spin-1 and spin-3/2 Ising system ferromagnet. *IEEE Trans. Magn.*, 38:2406–2408, 2002.
[23] A. Bobak, "The Effect of Anisotropies on the Magnetic Properties of a Mixed Spin-1 and Spin-3/2 Ising Ferri magnetic System," Physica A, Vol. 258, No. 1-2, 1998, pp. 140-156.
[24] E. Albayrak, "Mixed-Spin-2 and Spin-5/2 Blume-Emery Griffiths Model," Physica A: Statistical Mechanics and Its Applications, Vol. 375, No. 1, 2007, pp. 174-184.
[25] M. Keskin and M. Ertas, "Existence of a Dynamic Compensation Temperature of a Mixed Spin-2 and Spin-5/2 Ising Ferrimagnetic System in an Oscillating Field," Physical Review E, Vol. 80, No. 6, 2009.
[26] B. Deviren, E. Kantar and M. Keskin, "Magnetic Proper ties of a Mixed Spin-3/2 and Spin-2 Ising Ferrimagnetic System within the Effective-Field Theory," Journal of the Korean Physical Society, Vol. 56, No. 6, 2010, pp. 1738-1747.